Fabrication of Palladium Nanotubes and Their Application in Hydrogen Sensing

Shufang Yu, Ulrich Welp, Leonard Z. Hua, Andreas Rydh, Wai K. Kwok, and H. Hau Wang*

Materials Science Division, Argonne National Laboratory, Argonne, Illinois 60439

Received October 15, 2004. Revised Manuscript Received April 22, 2005

A new electroless plating method was used to deposit palladium nanotubes within the pores of track-etched polycarbonate membranes. The morphology of the deposited palladium nanostructures were characterized with the use of field-emission scanning electron microscopy (FESEM), energy-dispersive X-ray spectrometry (EDX), and transmission electron microscopy (TEM). The largely expanded surface area and granular nature of the nanotubes make them ideal for applications that require high surface area. One of the applications investigated here is hydrogen sensing. Palladium nanotubes excel in high sensitivity, low detection limit, and fast response times in hydrogen sensing compared to sputtered Pd thin film on glass. The response time ranges from a few seconds to tens of seconds depending on the concentration of hydrogen. The hydrogen sensing behavior can be understood with the Langmuir adsorption isotherm theory at very low hydrogen concentration. The high sensitivity and fast response time in the nanotube imbedded samples imply that the nanostructures create not only larger surface areas but also many more favorable sites for hydrogen adsorption to occur. These new nanostructured sensing elements are superior to the conventional thin film sensors especially in the low hydrogen concentration region.

Introduction

Nanotube structures have drawn much attention due to their unique physical properties and potential applications in separation systems, drug delivery, sensors, and catalysis.[1−6] In particular, palladium nanotubes are of considerable interest for catalysis, hydrogen storage, and sensor technology. Several methods have been used to prepare palladium nanotubes. For example, Xia's group[7,8] has synthesized Ag nanowires in solution and subsequently displaced Ag with Pd through a galvanic replacement reaction by refluxing Ag nanowires with palladium nitrate. During this reaction, only one palladium atom is generated for every two silver atoms oxidized, starting from an external reaction outside of the nanowires, which finally results in the creation of palladium nanotubes. This method limited the nanotubes' lengths to less than 2 μm, with any longer length resulting in only partial segments of the nanowires being converted to nanotubes. Template synthesis entails deposition of desired materials within nanosized cavities of a host, for example, within the pores of a porous membrane.[9−11] This method is very general because nearly any chemical synthesis method used to prepare bulk materials can be adapted to synthesize nanomaterials including metals,[12−15] polymers,[16−18] carbons and semiconductors.[19−22] In addition, the templates make it much easier to handle the entire synthesis process. Palladium nanotubes have also been synthesized with the template synthesis.[23,24] For example, ordered porous alumina membranes were first wetted with a solution containing polylactide and palladium acetate. Subsequent annealing of the membrane led to degradation of palladium acetate to form Pd.[24] However, this method often resulted in dispersed Pd nanoparticles instead of continuous nanotubes on the pore walls due to the removal of polylactide, which tends to form cavities. Hermann's group used a two-step procedure of forming copper nanotubes first and then displacing Cu with Pd to obtain palladium nanotubes.[23]

* To whom correspondence should be addressed. Telephone: 630-252-3461. Fax: 630-252-9151. E-mail: hau.wang@anl.gov.

(1) Kong, J.; Franklin, N.; Zhou, C.; Chapline, M.; Peng, S.; Cho, K.; Dai, H. *Science* **2000**, *287*, 622.
(2) Yu, S.; Lee, S. B.; Kang, M.; Martin, C. R. *Nano Lett.* **2001**, *1*, 495.
(3) Wirtz, M.; Yu, S.; Martin, C. R. *Analyst* **2002**, *127*, 871.
(4) Qi, P.; Vermesh, O.; Grecu, M.; Javey, A.; Wang, Q.; Dai, H. *Nano Lett.* **2003**, *3*, 347.
(5) Varghese, O. K.; Gong, D.; Paulose, M.; Ong, K. G.; Grimes, C. A. *Sens. Actuators, B−Chem.* **2003**, *93*, 338.
(6) Yu, S.; Lee, S. B.; Martin, C. R. *Anal. Chem.* **2003**, *75*, 1239.
(7) Sun, Y.; Mayers, B.; Xia, Y. *Adv. Mater.* **2003**, *15*, 641.
(8) Sun, Y.; Tao, Z.; Chen, J.; Herricks, T.; Xia, Y. *J. Am. Chem. Soc.* **2004**, *126*, 5940.
(9) Martin, C. R. *Science* **1994**, *266*, 1961.
(10) Hulteen, J. C.; Martin, C. R. *J. Mater. Chem.* **1997**, *7*, 1075.
(11) Martin, C. R.; Mitchell, D. T. *Anal. Chem.* **1998**, *70*, 322A.
(12) Brumlik, C. J.; Martin, C. R. *J. Am. Chem. Soc.* **1991**, *113*, 3174.
(13) Foss, C. A., Jr.; Hornyak, G. L.; Stockert, J. A.; Martin, C. R. *J. Phys. Chem.* **1992**, *96*, 7497.
(14) Menon, V. P.; Martin, C. R. *Anal. Chem.* **1995**, *67*, 1920.
(15) Nishizawa, M.; Menon, V. P.; Martin, C. R. *Science* **1995**, *268*, 700.
(16) Cai, Z.; Martin, C. R. *J. Am. Chem. Soc.* **1989**, *111*, 4138.
(17) Liang, W.; Martin, C. R. *J. Am. Chem. Soc.* **1990**, *112*, 9666.
(18) Parthasarathy, R.; Martin, C. R. *Nature* **1994**, *369*, 298.
(19) Klein, J. D.; Herrick, R. D., II; Palmer, D.; Sailor, M. J.; Brumlik, C. J.; Martin, C. R. *Chem. Mater.* **1993**, *5*, 902.
(20) Parthasarathy, R. V.; Phani, K. L. N.; Martin, C. R. *Adv. Mater.* **1995**, *7*, 896.
(21) Lakshmi, B. B.; Patrissi, C. J.; Martin, C. R. *Chem. Mater.* **1997**, *9*, 2544.
(22) Che, G.; Lakshmi, B. B.; Fisher, E. R.; Martin, C. R. *Nature* **1998**, *393*, 346.
(23) Hermann, A. M.; Ramakrishnan, P. A.; Badri, V.; Mardilovich, P.; Landuyt, W. *Int. J. Hydrogen Energy* **2001**, *26*, 1295.
(24) Steinhart, M.; Jia, Z.; Schaper, A. K.; Wehrspohn, R. B.; Gosele, U.; Wendorff, J. H. *Adv. Mater.* **2003**, *15*, 706.

10.1021/cm048191i CCC: $30.25
Published on Web 05/24/2005

Recently, hydrogen detection has aroused much interest with nanostructures related to palladium or new materials due to national priority—preparation of a future hydrogen-based economy. Hydrogen is a very clean and promising energy source, but before the adoption of a hydrogen economy, ultrasensitive hydrogen sensors are urgently needed for early detection of hydrogen leakage at any level. Commercial hydrogen sensors typically based on palladium thin films or Si MEMS devices are limited by their response time (tens of seconds) and physical dimension (inches). Dai's group[25] modified single-walled carbon nanotubes with a thin layer of Pd and developed a hydrogen sensor with good sensitivity at the 400 ppm H_2 level. While the art of handling individual nanotubes was elegantly demonstrated in this approach, the task of mounting each nanotube for mass application is simply daunting! Recently, a new material, titania nanotube,[5] has been prepared and used for hydrogen sensing. However, the lowest operating temperature for this sensor to have appreciable sensitivity is 180 °C. The fastest hydrogen sensor so far was developed by Penner's group.[26,27] Mesoscopic palladium wires were electrodeposited onto a highly oriented pyrolytic graphite surface and formed the basis for a hydrogen sensor. This type of sensor has very fast response time, but the detection mechanism depends on the volume expansion from Pd to PdH_x, and hence limits the detection to only approximately 1% hydrogen.

In this paper, we used a one-step direct electroless plating procedure to obtain continuous and granular Pd nanotubes for the first time. The advantages of the electroless plating technique to prepare nanostructures are easy deposition on complex shapes, large area, low cost, and a relatively simple procedure. The rough granular surface of the resulting palladium nanotubes makes it ideal for high surface area applications. The ideal hydrogen sensor should be easy to fabricate and handle, have fast response times, high sensitivity, and low detection limit, and operate at room temperature. The granular palladium nanotubes which we have fabricated with a direct electroless deposition method may entertain all these features. We describe the results of our preliminary investigations of hydrogen detection herein.

Experimental Section

Materials. The template membranes used in our studies were track-etched polycarbonate (PC) filters obtained from Poretics and coated with poly(vinylpyrrolidone) (PVP) to increase surface hydrophilicity. The membrane is 9 μm thick with nominal diameter and pore density of 600 nm and 3×10^7 pores cm^{-2}, respectively. Anhydrous $SnCl_2$, $AgNO_3$, trifluoroacetic acid, anhydrous methanol, $PdCl_2$, disodium EDTA, and hydrazine (N_2H_4) were obtained from Sigma-Aldrich and used as received. Hydrazine is an anticipated human carcinogen. It should be used in a well-vented hood with extreme care. Toxicity and disposal should be referred to its MSDS sheet.

Synthesis of Palladium Nanotubes. Before the one-step direct electroless deposition, the membrane was sensitized and activated, as described in detail, elsewhere.[14] Briefly, the polycarbonate membrane was first sensitized by immersing it in a solution containing tin chloride and trifluoroacetic acid, causing Sn^{2+} to bond onto the pore walls of the PC membrane. After the membrane was rinsed with methanol, it was activated in a solution of ammoniacal $AgNO_3$. A redox reaction occurs in which surface-bound Sn^{2+} is oxidized to Sn^{4+} and Ag^+ is reduced to Ag. The resulting Ag nanoscopic particles act as nuclei and catalysts for deposition and growth of palladium in the following electroless deposition. Finally, the membrane was rinsed with methanol followed by distilled water.

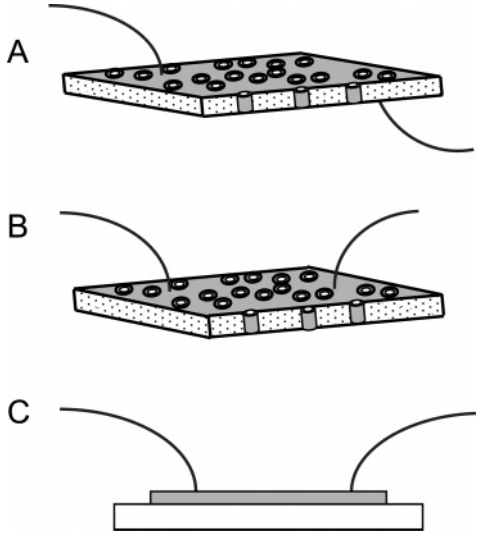

Figure 1. Schematic drawings of electrode geometry for hydrogen sensing. (A) Two Au wires on different faces of the nanotube membrane. (B) Two Au wires on the same face of the membrane. (C) Two wires on sputtered thin Pd film on a glass substrate.

For direct palladium electroless deposition, the activated membrane was transferred to a fresh solution containing 1 mM $PdCl_2$, 13 mM disodium EDTA, and 18 mM hydrazine (N_2H_4). In this solution, $PdCl_2$ is the palladium precursor, with hydrazine N_2H_4 as the reducing agent. The complexing agent (disodium EDTA) chelated with the palladium ions[28] forming $[Pd(EDTA)]^{2-}$ which allows the following reaction (eq 1) to be slowly carried out at room temperature on the pore walls and the surface of the membrane. In this way, the palladium nanotubes can span through the entire thickness of the membranes. After the deposition of Pd,

$$2[Pd(EDTA)]^{2-}_{(aq)} + N_2H_{4(aq)} + 4OH^-_{(aq)} \rightarrow 2Pd_{(s)} + 2EDTA^{4-}_{(aq)} + N_{2(g)} + 4H_2O_{(l)} \quad (1)$$

the membrane was rinsed with water and dried in air.

Characterization of Palladium Nanostructures. Field-emission scanning electron microscopy images (FESEM) and energy-dispersive X-ray spectrometer data (EDX) were obtained on an Hitachi S-4700-II field emission scanning electron microscope operating with an accelerating voltage of 10 kV. Transmission electron micrographs (TEM) and electron diffraction patterns were obtained on a Philips CM30T at 200 kV.

Hydrogen Sensing Experimental Setup. The sensing electrode geometry of the palladium nanotubes is shown in Figure 1. Arrays of palladium nanotubes were grown within the template membranes. With the aid of an optical microscope, two pieces of gold wires (diameter 30 μm) were attached to different faces of the membrane with silver paste (Figure 1A). In this configuration, the electrical

(25) Kong, J.; Chapline, M. G.; Dai, H. *Adv. Mater.* **2001**, *13*, 1384.
(26) Favier, F.; Walter, E. C.; Zach, M. P.; Benter, T.; Penner, R. M. *Science* **2001**, *293*, 2227.
(27) Walter, E. C.; Favier, F.; Penner, R. M. *Anal. Chem.* **2002**, *74*, 1546.
(28) Pan, X. L.; Xiong, G. X.; Sheng, S. S.; Stroh, N.; Brunner, H. *Chem. Commun.* **2001**, 2536.

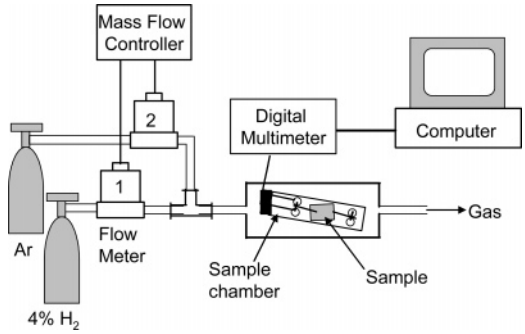

Figure 2. Schematic of hydrogen sensing experimental setup.

current must flow through the nanotubes and across the membrane. For comparison, two control experiments were conducted as well. First, two gold wires were attached on the same face of the membrane with the same lateral distance (Figure 1B) as in Figure 1A. Second, a 20 nm thick palladium was thermally evaporated on glass, and then two Au wires were attached on it also with similar lateral distance (Figure 1C). For the two control experiments, we probed the responses of the Pd thin films. The as-prepared samples were mounted onto a standard four-probe holder acting as a two-probe experimental stage with the sample's Au wires attached with silver paste to two of the four-probe electrical contacts.

A schematic diagram of the experimental setup used for the hydrogen gas sensing studies is shown in Figure 2. The two probe-contacted sample is sealed inside a small test-chamber to which a gas inlet and an outlet have been attached. Gas flow through the test chamber was controlled via a MKS mass flow controller to produce a flow rate of 400 SCCM (standard cubic centimeters per minute) for all measurements. The sample was connected to a computer-controlled Keithley 197 digital multimeter via a BNC-connector, and the electrical resistance across the sample was measured as the sample was exposed from an argon gas environment to one containing a fixed percentage of hydrogen gas, and then back to argon which defined one cycle. At least two cycles were performed for each sample. All data acquisitions were carried out with a LabView software program through a GPIB interface card. All measurements were conducted in a range of hydrogen concentration from 0.05% to 1%.

Results and Discussion

Figure 3A displays the field emission scanning electron micrograph (FESEM) of the membrane surface after electroless Pd deposition. Figure 3B delineates the resulting Pd nanotubes after they were released by dissolving the template membrane with methylene chloride and collected on a porous 200 nm anodic alumina filter. The wall thickness of the palladium nanotubes is fairly uniform and around 50 nm as shown in Figure 3C. For comparison, Figure 3D shows the SEM image of a Pd thin film on a glass substrate. The shiny Pd surface is very smooth with grain sizes less than 10 nm. Our Pd nanotubes, however, possess a highly granular surface, which is desirable for high surface area applications and enables our Pd nanotubes to reach a lower detection limit and higher sensitivity for hydrogen detection, as described below.

EDX analyses of samples in Figure 3A (surface of Pd deposited membrane) and 3B (palladium nanotubes collected on alumina filter) confirmed the obtained nanostructures were indeed palladium as shown in Figure 4. Both samples had very strong Pd signals at 2.838 keV (PdLa) and 3.010 keV

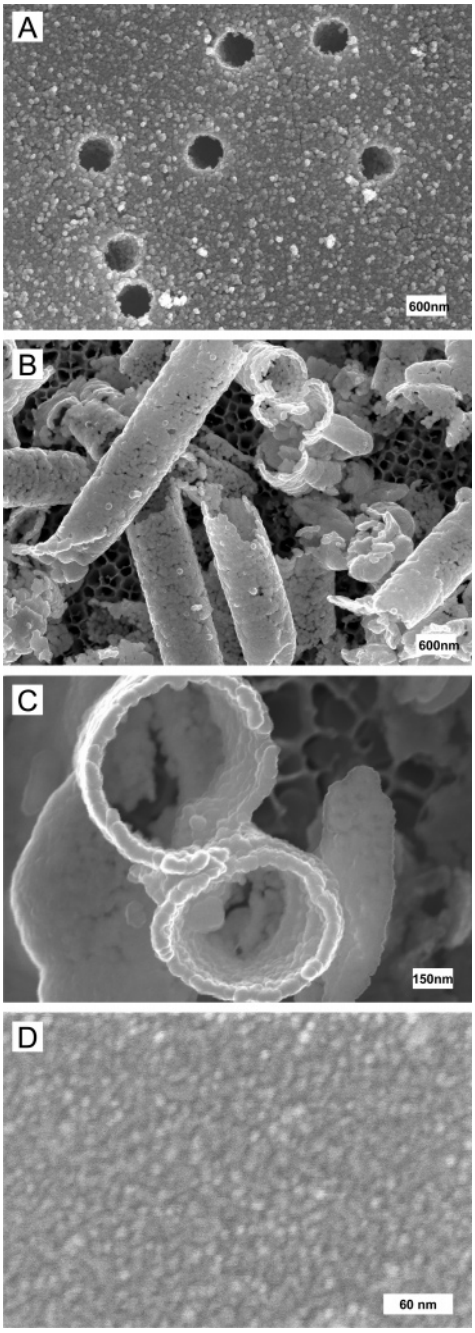

Figure 3. Scanning electron micrographs of a palladium nanotube membrane. (A) Surface of the Pd deposited PC membrane. (B) Palladium nanotubes collected on porous alumina membrane after dissolving away the template. (C) Top view of two collected palladium nanotubes. (D) Surface of a thin Pd film on a glass substrate.

(PdLb). In the collected palladium nanotubes (dotted line), significant oxygen (0.523 keV) and aluminum (1.490 keV) signals resulted from the aluminum oxide filter used to collect the released palladium nanotubes. Carbon signals (0.282 keV) in both samples came from the chamber environment; the stronger carbon signal in the sample from Figure 3A was due to the polycarbonate template membrane. EDX analysis of the released Pd nanotubes on a TEM grid using CM30 TEM with 200 kV showed strong PdKa and PdKb signals (not shown).

Figure 5A shows the TEM images of the resulting palladium nanotubes (insert is at a higher magnification with a 30 nm scale bar). After deposition, the Pd nanotubes were

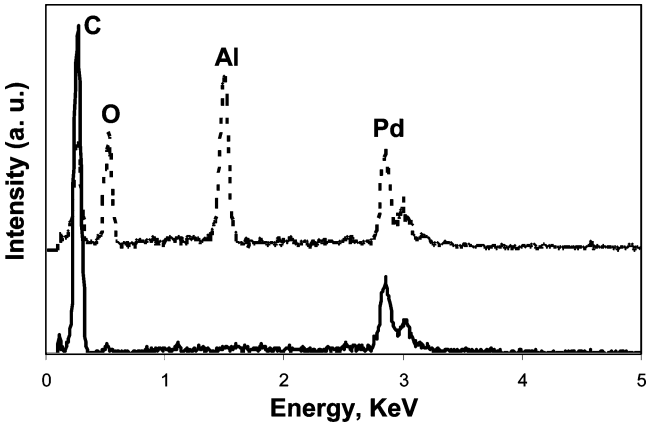

Figure 4. EDX spectra of the resulting nanostructures: solid line, sample in Figure 3A; dotted line, sample in Figure 3B.

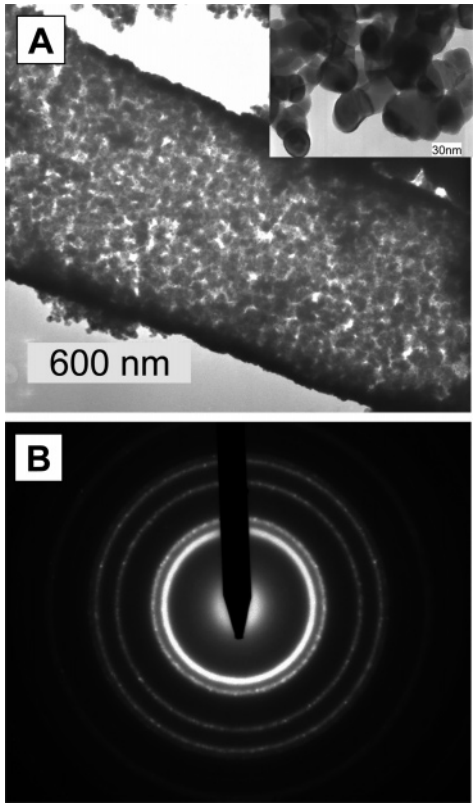

Figure 5. (A) TEM images of Pd nanotubes (insert is at a higher magnification). (B) Selected area electron diffraction of Pd nanotube.

released, rinsed, and collected on a TEM grid. The size of the Pd crystallites is around 32 ± 10 nm. Figure 5B shows the electron diffraction patterns obtained from a selected area of the sample. The Debye−Scherrer (ring) patterns demonstrate the Pd is polycrystalline. These patterns can be interpreted by relating the distances and angles in the crystal lattice via the Bragg Law (eq 2):

$$\lambda = 2d \sin\theta \tag{2}$$

For electron diffraction patterns the wavelength is small (at 200 kV, wavelength λ is only 0.02506 Å), and so θ is also small. Bragg law can be transferred to eq 3. where d is

$$L\lambda = \mathrm{d}r \tag{3}$$

the d spacing of a plane, r is the ring radius, L is the effective camera length, and λ is the wavelength of the electrons. $L\lambda$ is a camera constant, which is obtained by calibration with an aluminum film of known lattice parameters. The calculated (vs standard) d spacings of planes (111), (200), (220), (311), and (222) for Pd nanotubes are 2.2517 (2.2457) Å, 1.952 (1.9449) Å, 1.372 (1.3752) Å, 1.176 (1.1728) Å, and 1.120 (1.1228) Å, respectively, which is consistent with standard Pd (around 0.2% deviation). Consequently, the lattice constant of cubic Pd is 3.892 Å, consistent with the lattice constant (3.889 Å) of standard Pd α-phase. (All the standard Pd data are from 2003 JCPDS-No.89-4897.) No Ag line was observed.

PC membrane with imbedded Pd nanotubes is expected to give larger surface area. A simple surface area calculation for the Pd nanotubes in the PC membrane vs a continuous Pd thin film indicates that, for a 0.5 × 0.5 cm^2 sensing element, the surface area with nanotubes is ∼7 times larger (based on known pore density of 3×10^7 pores cm^{-2}, membrane thickness of 9 μm, and pore diameter of 600 nm). This calculation assumed the surface of Pd nanotubes to be smooth; the actual surface area is much larger due to the rough surface.

Electrical resistance across two connecting Au wires on each sample was measured with the experimental setup shown in Figure 2. For resistance detection, the current will flow along a conduction pathway but not the entire surface. To probe the nature of the Pd nanotubes, we first estimate the resistances of all three samples. For smooth palladium sample with uniform geometrical shape, the resistance of the sample can be calculated based on the following equation.

$$R = \rho\, l/A \tag{4}$$

where R is the calculated resistance (Ω), ρ is the resistivity of Pd (1.05×10^{-5} Ωcm), l is the sample length (cm), and A is the cross sectional area of a conduction pathway (cm^2).[29] The resistances of samples with configurations B and C can be calculated as thin rectangular films (0.15 × 0.50 cm^2 with 50 and 20 nm thickness, respectively). For calculation, sample A consists of the same rectangular film as that of B plus a single nanotube (600 nm diameter, 50 nm thick, and 9 μm long). The measured vs calculated (in parentheses) resistances of samples A, B, and C at ambient temperature are ∼700 (17.9), 13 (7.0), and 142 (17.5) Ω, respectively. While measured resistance gives a good agreement with the calculated value for sample B, sample C gives a somewhat higher measured value likely due to the glass substrate with an uneven surface and the granular nature of the Pd film (with grain size less than 10 nm, Figure 3d). However, the measured resistance for sample A is nearly 40 times larger than the calculated one. This result indicates unusually high resistance due to the nanotubes and is consistent with the *highly* granular surface of the Pd nanotubes as revealed in Figure 5a. The high contact resistance between the granules in the Pd nanotubes is likely the reason for the overall high resistance in sample A.

For sensor testing, each sample was first exposed to argon gas to obtain a baseline, then to a desired percentage of

(29) Kittel, C. *Introduction to Solid State Physics*; John Wiley & Sons: New York, 1986.

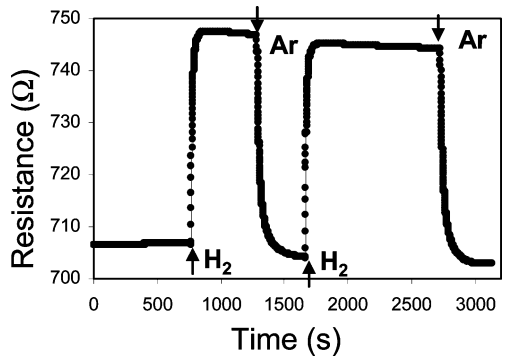

Figure 6. Resistance versus time for the sample in Figure 1A at 0.5% H_2.

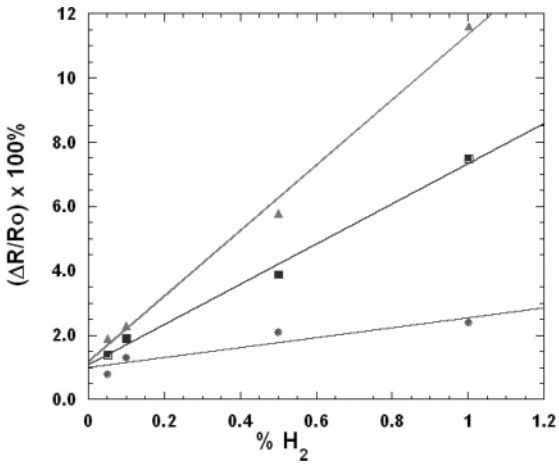

Figure 7. Sensitivity versus hydrogen concentration for three samples in Figure 1 (triangles 1A, squares 1B, and circles 1C).

hydrogen gas, and then back to argon gas which completed one cycle. A typical time-dependent resistance graph is shown in Figure 6, for the sample in Figure 1A with the concentration of 0.5% hydrogen in Ar. Exposure of the sample to hydrogen shows a prompt increase in the sample resistance. When Pd is exposed to hydrogen, hydrogen molecules dissociate into hydrogen atoms which diffuse into the Pd lattice and react with Pd to form palladium hydride (PdH_x). The resistivity of PdH_x is higher than that of pure Pd.

We used sensitivity and response time to compare the hydrogen sensing performance of different samples. The sensitivity S is defined as the percentage of resistance change by the formula

$$S = (R_S - R_0)/R_0 \times 100\% \quad (5)$$

where R_0 is the resistance of the sensor in the presence of argon only and R_S is the resistance after exposure to a fixed percentage of hydrogen. The percentage of resistance change ($\Delta R/R_0$) takes into account the dimensions of the sample and allows comparison between different samples. The response time (τ) is defined as the time needed for the sensor to reach e^{-1} (or ~36.8%) of the total change for a given concentration of hydrogen. The sensitivity of all three samples with percentage of hydrogen exposure is shown in Figure 7.

The palladium nanotube sample with two probes on different faces of the membrane (Figure 1A) has the highest sensitivity at all concentrations. At a hydrogen concentration of 1%, the sensitivity is as high as 11.6. Even at 500 ppm (0.05%) H_2, the sensitivity is around 2. The linear relationship between the electrical resistance change and hydrogen content has been reported in the literature.[30] It can be compared with the Langmuir adsorption isotherm theory.[31] The resistance increase ($\Delta R/R_0$) for a good approximation is proportional to the fraction of surface that is covered by hydrogen (θ), and θ can be described as follows:

$$\frac{\Delta R}{R_0} \propto \theta = \frac{Kp}{1 + Kp} \quad (6)$$

where K is an equilibrium constant defined as the adsorption constant (k_1) divided by the desorption constant (k_{-1}) and p denotes gas pressure which in the current experiment is equivalent to the hydrogen partial pressure. At low hydrogen partial pressure ($Kp \ll 1$), which was the condition in our experiments, eq 6 simplifies to $\Delta R/R_0 \approx Kp$. The slopes of the three samples are $K_{1A}:K_{1B}:K_{1C} = 10.17:6.27:1.54$, respectively. The differences between these values are outside of measurement uncertainty. All samples are chemically the same but probed differently. In addition, both A and B contain nanotubes, while sample C is a smooth thin film with no nanostructure. With sample configuration A, nanotubes are directly probed. Detailed kinetic analysis is beyond the scope of this article and the result is only phenomenologically explained as follows. Since there is no material difference and for a smooth surface both percentage resistance change ($\Delta R/R_0$) and fraction of adsorbed surface (θ) are not affected by the sample size, the result of a larger K ($= k_1/k_{-1}$) implies more favorable adsorption (larger k_1) and less favorable desorption (smaller k_{-1}) with the trend following A > B > C. The adsorption process is known to be sensitive to specific crystallographic surfaces and active sites.[31] Large K_{1A} may be due to the highly granular nature of the nanotubes that creates not only larger surface area but also many more favorable sites for the adsorption to occur. The built-in nanoporous structure, larger surface area, and rougher surface likely lead to higher sensitivity in samples A and B.

Figure 8 shows the response time versus hydrogen concentration for all three samples. Surprisingly, sample 1A also has the fastest response time. The effect is most pronounced at low concentrations (below 0.1% H_2). At the 500 ppm H_2 level, the response time for nanotubes based sample A is 1 order of magnitude less than that of the conventional thin film based sample C. The response times are more comparable for all three samples at higher concentration of hydrogen (1%). This unusual result points to a unique advantage for very low concentration detection from nanotubes-based sensors. Since the response time (τ) is a measure of how fast the resistance rises to e^{-1} (or 36.8%) of the total increase, the inverse of the response time ($1/\tau$) corresponds to the initial hydrogen adsorption rate. Figure 8 is plotted again as $1/\tau$ vs hydrogen concentration and is shown in Figure 9.

As shown in Figure 9, for sample 1C, the initial hydrogen adsorption rate ($1/\tau$) follows a linear relationship with

(30) Lewis, F. A. *The Palladium Hydrogen System*: Academic Press: New York, 1967.
(31) Laidler, K. J. *Chemical Kinetics*; McGraw-Hill Book Company: New York, 1965; p 260.

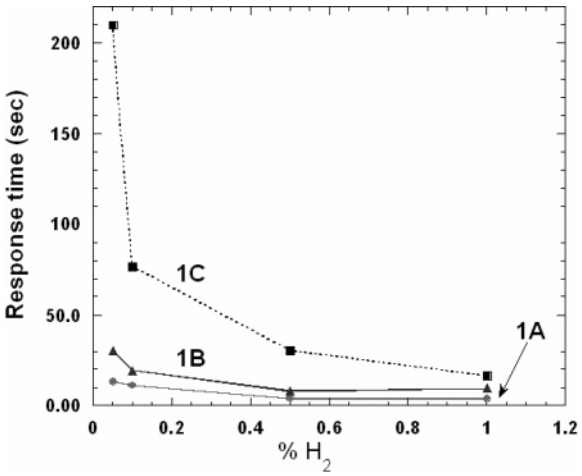

Figure 8. Response time versus hydrogen concentration for three samples in Figure 1. The lines between data points are guides for the eye.

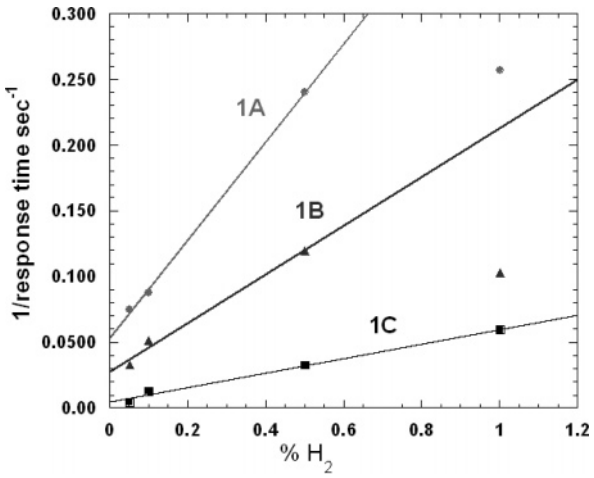

Figure 9. $1/\tau$ (response time) against hydrogen concentration for samples 1A, 1B, and 1C. Only three data points each were used for samples 1A and 1B for the linear fit (see text for details).

hydrogen concentration. For samples 1A and 1B, the adsorption rates follow a linear correlation with hydrogen except at higher concentration of 1%. This behavior can also be understood with the Langmuir adsorption theory. At the initial stage of the measurement, the rate of hydrogen adsorption is $r = k_1p(1 - \theta)$, where $1 - \theta$ indicates the fraction of surface that is not covered by H_2. Since θ is negligible at the initial stage (or $Kp \ll 1$), the adsorption rate is approximately $r \approx k_1p$. This condition will no longer hold true for samples 1A and 1B with large K and at a higher H_2 concentration (p) of 1%. In other words, θ (fraction of H_2 covered surface) quickly becomes non-negligible, and the adsorption rate, r, decreases. Larger initial adsorption rates (r) for samples 1A and 1B can be understood by their larger adsorption constants (k_1, see discussion associated with Figure 7), due to their nanoporous structure, larger surface areas, and the rougher surfaces.

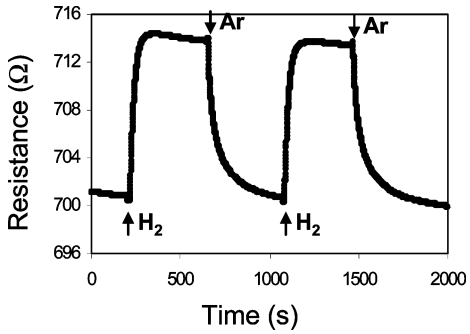

Figure 10. Resistance versus time for the sample in Figure 1A at 0.05% (500 ppm) H_2.

Conclusion

We have demonstrated a new and facile approach to synthesize palladium nanotubes. The granular surface of the nanotubes is preferred for the high surface area requirement, which contributes to high sensitivity and low detection limit for hydrogen sensing. This sensor has many advantages. It is easy to make and handle, is inexpensive, can be operated at room temperature, and has low power requirements. A detection limit as low as 500 ppm has been demonstrated. Even at this low concentration, very good resolution with sensitivity up to 2 is shown in Figure 10. Since the sensing element parameters such as pore diameter and density are far from optimized, we can extend the detection limit to much lower concentration. The responses of nanostructured membranes exposed to other gases such as ammonia, oxygen, and methane is also an interesting subject. Higher pore density of ordered alumina porous membranes will also be investigated in the future. Since porous alumina membranes are easily etched in acidic and basic solutions, a neutral or close to neutral environment will be necessary to obtain Pd nanotubes. The direct electroless Pd deposition process (pH 6.1) presented in this article may be adapted. However, because strong acidic solution is used during sensitization, appropriate sensitizing agents or modified conditions are needed for porous alumina membranes. A new deposition procedure will be the subject of future studies.

Acknowledgment. Work at Argonne National Laboratory as well as measurements with Field Emission Scanning Electron Microscopy carried out in the Electron Microscopy Center at the Argonne National Laboratory are supported by U.S. DOE, the Office of Basic Energy Sciences, Division of Materials Science, under Contract No. W-31-109-Eng-38. S.Y. and H.H.W. would like to thank Russell E. Cook for helpful discussions on electron diffraction. L.Z.H. is an undergraduate student research participant sponsored by the Argonne Division of Educational Program from the University of Illinois, Urbana-Champaign.

CM048191I